A STUDY OF NANOMATERIALS WITH NANOSTRUCTURES WITH DIFFERENT TECHNIQUES

K. Vandana Devi, Dr. Chaudhari Kishor Gopalrao
Department of Physics, College- Malwanchal University, Indore

ABSTRACT

To improve their stability, reduce their immunogenicity and toxicity, and lengthen their in vivo circulation time, enzymes are immobilized within a nanomaterial. Some enzymes, whether they're used in medicine or not, benefit from immobilization methods. Synthetic polymers can be composited to study enzyme immobilization, especially for medical enzymes like lysozyme. The use of clay-based PNCs as carriers for regulated drug delivery holds much promise. The drug delivery systems used a wide range of clays, including saponite, kaolin, laponite, montmorillonite (MMT), and halloysite. It's safe to say that MMT has become the natural material of choice for the majority of applications. It's superior qualities include high availability, high internal surface area, and the capacity for high adsorption, swelling, and biocompatibility. Consequently, the FDA has deemed this drug to be GRAS. Applications in biomedical engineering involving composite nanomaterials span the gamut from disease diagnostics to therapy. Proteomic profiling can benefit from the integration of various multidisciplinary approaches, especially when trying to locate biomarkers. The use of nanomaterials in nanobiotechnology has aided in the 3-D printing of cell culture scaffolds, medical implants, drug design and delivery systems, biosensors for disease diagnosis, and medical imaging. Nanotechnology's parallel applications, integration, and automation are especially useful in biomedical technologies like point-of-care diagnostic kits, lab-on-a-chip technologies, and so on. The following sections focus on the applications of nanocomposites in the medical field, including biosensors, medical imaging, controlled drug delivery, and surgical implants.

DOI Number: 10.14704/nq.2022.20.13.NQ88334 Neuro Quantology 2022; 20(13):2675-2684

1. INTRODUCTION

The majority of these strategies take into account the interaction between biological beings and nanostructured materials. These nanoparticles are a very attractive candidate for application in the diagnosis, therapy, and regeneration of dysfunctional biological systems due to their ability to systematically modify their characteristics by regulating their structures and properties at the nanoscale. More than a few nanostructures have been studied for their potential as biosensors. These structures can take many different shapes, such as thin films, nanotubes, nanofibers, nanorods, and NPs. Using nanomaterials in biosensors paves the way for several innovative transduction advances that can be put to use in the in vivo research of a wide variety of substances. Nanotechnologies consider the use of biosensors and the biomolecules and processes that rely on them to create novel materials devices, nanomachines, and potentially even nanorobots. It is possible that modern cellular and sub-cellular nanodevices will be convincing in logical and medical applications, giving scientists and doctors one of the most formidable instruments imaginable to solve intractable problems, treat human illness, and address the health issues associated with aging. Considering these factors, a number of review articles have elaborated on the fundamentals of nanomaterial design from a variety of perspectives. Drug formulations for the treatment of specific populations (such as children), worldwide evaluations of nanotechnology, the current status of nanorobotics in medicine, specific applications of nanomaterials (such as antioxidants for cancer treatment), the incorporation of nanomaterials into bio imaging technologies, skin-contact nanoelectrodes, subcellular nanodevices, and so on are all examples. Outside of the typical, small-scale laboratory experiments, however, there is a

dearth of critical analysis that specifically disseminates the relevant knowledge for the design of NPs' shapes and sizes as well as their synthesis methodologies and characterisation techniques for commercial biomedical applications. We attribute this void to the numerous obstacles presented by the mass production of nanomaterials for medical uses. Defining a preparation procedure that can be scaled up enough to pay the expense necessary for pursuing volume markets is one way to overcome the difficulty of mass-producing nanomaterials at a reasonable price. Also, it's not easy to hand over the nanomaterials in a predetermined structure for incorporation into the assembling form, which is why these factors must be taken into account.

CLASSIFICATION OF NANOMATERIALS

As the nanoscale is defined as the "length range approximately from 1 to 100 nm," nanomaterials are "materials with any outward dimension in the nanoscale or having internal structure or surface structure in the nanoscale." Materials having a nanoscale structure have been shown to have superior magnetic, optical, electrical, and mechanical capabilities compared to their bulk counterparts, prompting a renewed focus on the controlled synthesis of nanostructured materials with a predetermined morphology. Nanomaterials can be broken down into four distinct categories based on how many dimensions they have: zero, one, two, and three. The NPs, quantum dots, and nanocrystals were all thought to exist in a single dimension. One dimensional structures include nanofibers, nanorods, nanoribbons, and nanowires, whereas two dimensional structures include thin films and nanorods. The colloids and fullerenes with the most complex structures are the ones with a three-dimensional nanostructure.

According to where they were produced, nanomaterials can be classified as either metallic, nonmetallic, or biodegradable (Fig. 1.). Synthesized from their bulk components, these materials can be coupled with antibodies, ligands, and medicines of interest by the use of different functional groups, allowing for a wide variety of uses in biotechnology. Ball milling, plasma arcing, and vapor destination are all examples of top-down approaches to synthesizing nanomaterials from bulk materials; bottom-up approaches like sol-gel and electrodeposition have not been used on a large scale in commercial applications.

Metallic Nanoparticles

Metallic nanoparticles (NPs) are characterized by high optical absorption due to a localized surface effect known as plasmon resonance; these NPs are being extensively studied for potential new medical applications. Many useful applications can be built upon the broad absorption band in the visible region of the electromagnetic spectrum that metal NPs like gold, silver, and copper possess. Many different metals have been investigated for potential medical applications, including gold, silver, and iron NPs. Iron oxide nanoparticles have a wide range of potential uses, including as MRI contrast agents, in hyperthermia therapy, for drug delivery, for gene delivery, and in bioimaging. While gold (AU) NPs are used in bioimaging, photothermal therapy, and drug delivery, silver (Ag) NPs are used for a wide variety of medical applications, including drug delivery, wound dressing, antimicrobial agents, and cancer therapy. Because of their ability to produce reactive oxygen species, zinc oxide NPs have recently found use as antimicrobial and anticancer agents, despite their more commonplace history of service in the paint and cosmetics industries. Synthesized NPs containing cadmium and copper have also been put to use in a number of fields of medicine.

Classification of nanomaterials

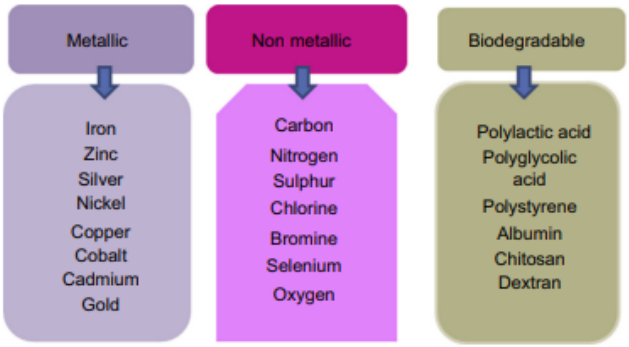

FIG. 1 Classification of Nanomaterials.

Nonmetallic/Inorganic Nanoparticles

The improved imaging and drug transport characteristics of nonmetallic and inorganic NPs have led to their widespread use in a variety of biomedical applications. Among the nonmetals, carbon has the widest range of potential uses in the biomedical sector, including drug delivery, bioimaging, tissue engineering, and biosensing. Biosensors, drug delivery vehicles, and tissue engineering all made use of single-walled multi-carbon nanotubes (CNTs). The drug delivery system also made use of fullerenes, which are composed of 60 carbon atoms and have a spherical shape. Modifying the properties of carbon nanotubes (CNTs) by adding elements like boron, nitrogen, or fluorine can have profound effects on fields like drug delivery and medical imaging. Mesoporous silica NPs are appealing carriers for drug delivery due to their high surface area and drug carrying capacities as well as the ease with which they can be synthesized, chemical stability, and biocompatibility. Nanoscale calcium phosphate is widely used in tissue engineering applications such as prosthetics and scaffolds.

Biodegradable Nanoparticles

The topic of nanodrug delivery makes extensive use of biodegradable nanomaterials. Polymeric materials are a safer choice because they degrade into harmless byproducts and are removed by the body's own systems. Because of their diversity in nature and function, natural and synthetic nanomaterials are employed for drug delivery, vaccine distribution, cancer therapy, and diagnostics. Because of their better biocompatibility, encapsulation, and drug release profile, biodegradable NPs have found widespread use in a range of drug targeting, medicinal, and other biological applications. They are non-toxic, biocompatible, and are removed naturally by the body, making them perfect for use in medicinal applications. Compounds of degradation are formed from hydrolyzed materials; these can be disposed of along with CO2 and water. There is a wide range of potential uses for biodegradable NPs, which can be broken down into two categories: natural and synthetic.

Biodegradable polymers can be broken down into three classes: agropolymers, chemically generated polymers, and microbially produced polymers. Natural polymers are either produced naturally or manufactured by organisms during their life cycles. Biodegradable polymers are widely used as scaffolds in tissue engineering and drug delivery vehicles, and the most common form are synthetic polymers since they can be cheaply produced in a lab. Synthetic polymers have several applications, including scaffolds, stents for wound therapy, and medication delivery. Natural biodegradable polymers such as chitosan, albumin, dextran, and lectin have been used as drug delivery vehicles in recent years. Polyaminosaccharide chitosan, produced by deacetylation of chitin, a polymer found in the shells of crustaceans, is the second most widely used polymer, following cellulose.

2. LITERATURE REVIEW

Gajanan, K., & Tijare, S. N. (2018) Materials with grains on the order of a billionth of a meter in size are referred to as nanomaterials. They exhibit extremely appealing and helpful characteristics that can be utilized in a wide variety of structural and non-structural applications. Nanomaterials have the potential to be used in a wide variety of contexts due to their superior chemical, physical, and mechanical properties, such as in next-generation computer chips, more lethal kinetic energy (KE) penetrators, and more effective insulation. High-definition television phosphors, inexpensive flat-panel displays, sharper and sharper cutting tools, less waste, less pollution, higher strength-to-weight ratios, Batteries, high-intensity magnets, highly sensitive sensors, and more fuel-efficient motors are only a few examples of the technological advancements that have led to the modern More powerful and compact weapon systems, aeronautic additives with enhanced performance characteristics, A satellite with a longer lifespan. Medical implants that last longer; ductile, machineable ceramics; large electrochromic display.

Khot, L. R., Sankaran, S.et al,(2012) Technological progress has enabled the production of nanoparticles in a plethora of shapes and sizes. These discoveries pave the way for further engineering to build unique traits that can be applied in several settings. Health care, environmental research, and the food business are just few of the fields where nanomaterials

have been put to good use without any negative effects. However, its potential uses in agriculture, especially in plant protection and agricultural production, have just been touched by researchers. Nanoparticles have shown promise in preliminary studies for their potential to aid in a variety of agricultural processes, including seed germination and growth, plant protection, disease identification, and pesticide/herbicide residue detection. This article gives a general overview of how nanomaterials may be used in farming in the future.

Gao, J., & Xu, B. (2009) Research into nanobiotechnology (also known as bionanotechnology) has risen in recent years in response to the explosive growth of this field. One of the most intriguing and important areas of nanobiotechnology is the use of nanomaterials inside cells for a wide variety of purposes, from imaging and tracking individual cells to combating cancer. We present case studies of various nanomaterials in action within cells and discuss the difficulties and future prospects for their use in biomedicine. In this article, we'll take a look at how various nanomaterials have been used within living cells.

Mandal, G., & Ganguly, T. (2011) As a science that draws from engineering, physics, chemistry, and biology, nanotechnology encompasses a wide range of tools. Nanotechnology is a rapidly developing area of science and technology that holds great promise for enhancing human health care and the prevention and treatment of disease. Nanotechnology's potential medical and physiological applications imply the development of novel materials and devices capable of highly targeted interaction with biological systems at the subcellular (or molecular) level. This has the potential to be applied in the clinic to target specific cells or tissues for maximum therapeutic benefit with little risk. This article provides an overview of nanotechnology, including its primary scientific and technical aspects and some of its possible applications.

3. METHODOLOGY

Production in algae

With its low cost and little impact on the environment, this method can be used as a viable alternative to traditional chemical and physical processes for creating nanoparticles. In addition, algae are able to absorb large amounts of metals. Marine algae and other biological sources have been proven to catalyze certain chemical reactions. This ability is crucial to developing practical and cutting-edge biosynthetic strategies. According to research using algae extract, the transformation of yellow to brown can be used to detect the conversion of silver ions into silver nanoparticles. Furthermore, it was seen that the time of incubation was directly related to the increase in the intensity of the brown coloration of the silver nanoparticles (which reached its deepest at 32 hours). Synthesis of silver nanoparticles was achieved via reduction of silver nitrate in aqueous solutions using powdered and solvent-extracted Padina pavonia. In addition, the produced nanoparticles were small in size, formed quickly, and exhibited high stability. bioreduction of silver ions induced by Spirogyra varians leads to the formation of silver nanoparticles.

Production in yeast

Some yeasts have been shown to be able to synthesize silver nanoparticles. Producing silver nanoparticles using yeast is not only cheap but also harmless to the environment. After adding Ag+ ions to the yeast culture, it was seen that the colorless sample gradually changed to reddish-brown over the course of incubation. Additionally, the solution's color shifted to a deep reddish-brown. the formation of nanoparticles outside of cells by a silver-tolerant yeast during exponential growth in the presence of soluble silver.

Synthesis based on DNA

The synthesis of silver nanoparticles can be facilitated by DNA acting as a reducing agent. DNA acts as a template stabilizer due to the high affinity of silver ions with DNA base pairs. The DNA base pair between the phosphate group at position 7 and the guanine group at position 7 was found to contain silver nanoparticles that had been artificially synthesized. Silver nanoparticles were synthesized using DNA from calf thymi, according to another study.

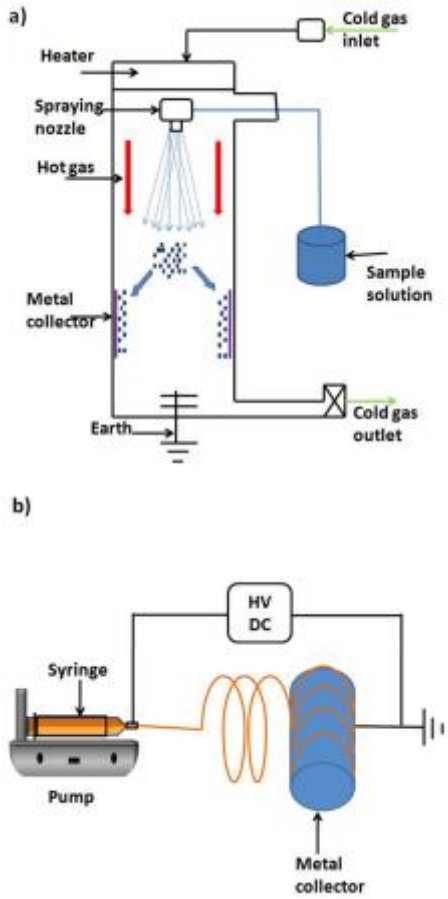

Figure 3. Schematic diagrams of (a) spray dryer and (b) electrospinner.

Beads in electrospraying separate from the cone and splash onto the objective because of the high quality of the electric field and the low viscosity of the solution. Electrospinning is a process where a fiber is released from the tip of a cone by applying a high voltage to the polymer. Many experiments in the areas of biomaterials and drug delivery systems have used electrospinning technology to successfully create nanofibres with smart properties. Bioactivity and antimicrobial efficacy of this wound dressing were demonstrated in vitro. Also mentioned was the use of a ciprofloxacin-loaded nanomembranous patch for the treatment of diabetic foot ulcers. The research group led by co-author Das modeled a membrane bioreactor that could be used with membranes created with the electrospinning method. Solute diffusion through these membranes in various media, such as water and cell culture medium, has also been the subject of laboratory experiments conducted by his team.

Laser Ablation Method

Recent years have seen a dramatic increase in the use of LASER by synthetic chemists for the purpose of creating nanomaterials, as this technology is rapidly developing and finding applications in virtually every area of scientific inquiry. As a result, laser ablation is a promising technique for developing and fabricating highly controlled, contaminant-free AuNPs. Intensity-modulated LASERs can be produced from a variety of different sources. Figure 4 shows a LASER system in which Q-switched Nd:YAG serves as the LASER source and dichroic mirrors, which are polished surfaces, direct the beam. Flask is home to the gold precursor. The Au precursors were subjected to intense LASER bombardment, which resulted in the formation of AuNPs. In addition, the laser ablation technique is a highly beneficial way to manufacture AuNPs in toluene. A 9 ns laser pulse at a repetition rate of 10 Hz is produced by irradiating a gold plate doused in toluene with a 1064 nm Nd:YAG laser. There's a yellow-amber hue to the solution that fades to yellow by the conclusion. When synthesized in DMSO, AuNPs also produce a red hue. As the agglomeration of nanoparticles can be dominated by their high surface energies, size control is always a concern when working with AuNPs, despite the fact that laser ablation makes it easy to change or reduce their size and morphology.

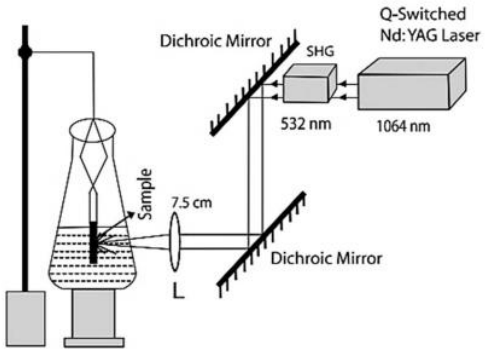

Figure 4. Fabrication setup of AuNPs through Laser ablation technique

4. RESULTS AND DISCUSSION

At a vacuum of 5 107 Torr, powdered CdSe or ZnSe (Merck, "Suprapure") and glassy GeS2, SiO, or Se were sequentially thermally evaporated from two separate tantalum crucibles. Between braces are numbers that indicate how quickly each set of layers was deposited. Multilayer structures consisting of GeS2SiOx=CdSe and Se/CdSe were fabricated, with a 3.5 nm, 5.0 nm, and 10 nm layer thickness, respectively. SiOx=ZnSe MLs had the following layer thicknesses: distances of 6.0 nm/10 nm, 6.0 nm/7.0 nm, 5.0 nm/5.0 nm, 3.5 nm/3.5 nm, and 2.5 nm/2.0 nm are all possible. Total ML thickness was in the range of 0:19:20:22 mm, and ML period (defined as sum of thickness of both kinds of layers in each ML) ranged from 4.5 to 20 nm. During deposition, the nominal layer thickness and deposition rate were monitored by two calibrated quartz moni tors (type MIKI-FFV). Substrates of non-heated Corning 7059 glass were used. Each layer of a multilayer structure was fabricated using a sequential deposition process. Substrates are rotated at a rate between 8 and 20 cycles per minute, with just 1/12 of each cycle spent over the source. where W is the width of the surface (as defined by root mean square surface variations, Rms), l is the length over which the roughness is measured, t is the amount of time that has elapsed (typically proportional to the thickness of the layer), a and b are the exponents of the roughness and growth, and z 14 a=b. As a result, the surface roughness can be quantified for sufficiently short lateral lengths by the root mean square of the surface fluctuations, where N is the number of data points of the AFM profile, hi I 14 1 to N) are the data points describing the relative vertical height of the surface, and hhi is the mean height of the surface.

$$Rms = \left\{ (1/N) \left[\sum_{i=1}^{N} (h_i - \langle h \rangle)^2 \right]^{1/2} \right\},$$

The height-height correlation function gx 14 fh12hx l hx2 ig1=2 can also be used to calculate roughness correlations across a distance l. since they are essentially the same picture. Rms values were calculated from AFM profiles of all MLs, characterizing the surface roughness at two length scales (250 nm2 and 3:4 mm2) in this investigation.

Figs. 5 and 6 show three-dimensional (3D) AFM images of SiOxð6 nmÞ=ZnSeð10 nmÞ,GeS2ð10 nmÞ=CdSe ð10 nmÞ and SiOxð10 nmÞ=CdSeð10 nmÞ multilayers, respectively. A first look at the figures shows that the surface morphology of the GeS2=CdSe and SiOx=CdSe MLs is quite similar with a large lateral size of the surface fluctuations. The observed similarity indicates that most likely the surface roughness of the nanocrystalline .CdSe sublayers is the dominant factor creating the surface roughness of these MLs. The surface of the SiOx=ZnSe ML is significantly smoother than that of

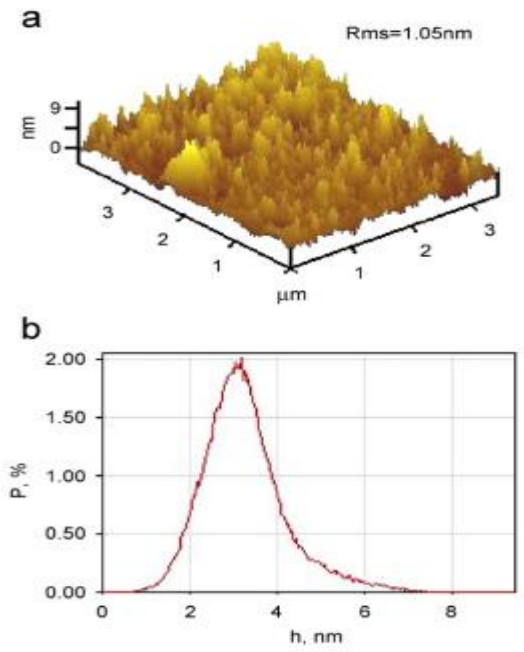

Fig. 5 Three-dimensional AFM image (a) and height histogram (b) of the surface roughness a SiOxð6 nmÞ=ZnSeð10 nmÞ multilayer.

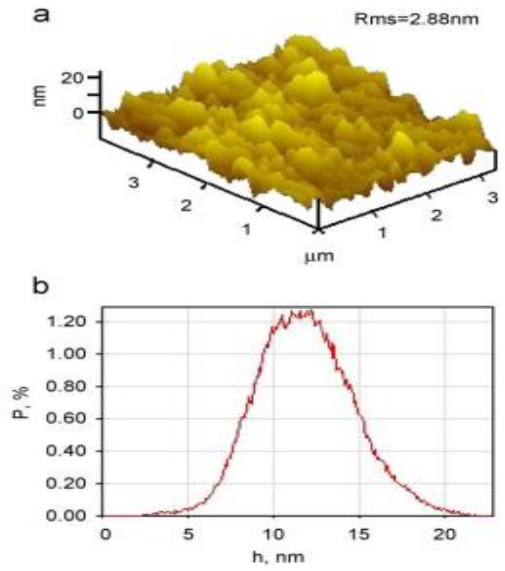

Fig. 6 Three-dimensional AFM image (a) and height histogram (b) of the surface roughness a GeS2ð10 nmÞ=CdSeð10 nmÞ multilayer.

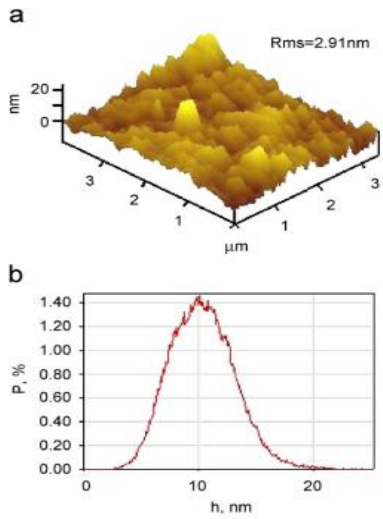

Fig. 7. Three-dimensional AFM image (a) and height histogram (b) of the surface roughness a SiOxð10 nmÞ=CdSeð10 nmÞ multilayer.

ZnSe sublayers should be smoother than CdSe ones because the CdSe-based MLs are rougher and the lateral size of the surface roughness is much smaller. The surface roughness of these three samples was measured at a scale of 3:4 4 mm2, and the resulting height histograms are shown in Figs. 8. The greatest heights of 22 and 7 nm are reached in the CdSe and ZnSe-based ML samples, respectively, however the histograms of the former are larger. SiOx=ZnSe, GeS2=CdSe, and SiOx=CdSe ML have all been measured to have Rms values of 1.05, 2.88, and 2.91 nm, respectively. Consequently, the height histograms and Rms values both provide quantitative confirmation that the surface roughness of the ZnSe-based ML is much lower than that of the CdSe-based ML.

The Rms values determined for each sample type are displayed in Fig. 7. Surface roughness of ZnSe-based MLs is seen to grow from Rms 14 0:5 nm to Rms 14 1 nm with increasing ML period from 4.5 to 17 nm b 0:72; nevertheless, it is still around three times smaller than the roughness of CdSe-based MLs for all thicknesses. There is no evidence of a consistent rise in roughness with layer thickness in the data obtained for CdSe-based MLs. Furthermore, the Rms values of MLs with SiOx, GeS2, or Se as the second material do not significantly differ, lending credence to the idea that CdSe sublayers play the dominant role.

AFM studies of the surface evolution of CrN=Si3N2 nanocrystalline/amorphous MLs deposited by magnetron

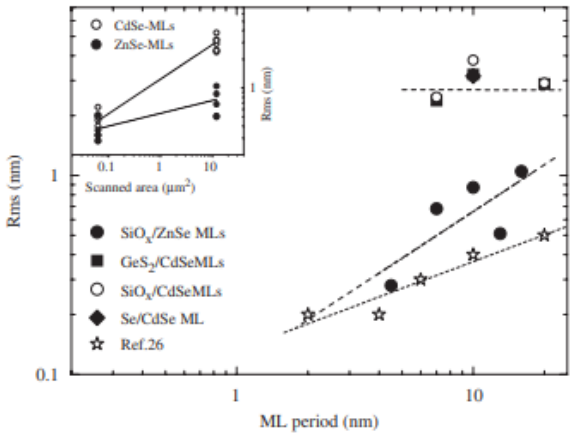

Fig. 8 Root mean square surface roughness (Rms)

All MLs analyzed on a 3:4 scale, represented here as length in millimeters per second, vs their average period. CdSe-based MLs are shown to have a Rms that is three times higher than that of ZnSe-based MLs. RMS against scanned area in the inset. The dotted lines are meant to be used as visual aids.

The 250 nm length scale Rms values of all MLs are displayed in fig 9 . Those obtained for the 4 3:4 mm2 scale are, predictably, smaller. It is worth noting that the difference between the surface roughness of CdSe and ZnSe-based MLs is not nearly as large as it was for the '4 mm' scale. This finding could be explained by the malleable

structure of amorphous materials, where the lattice mismatch at interfaces has less of an impact on the interface thickness over short lateral distances (in our case SiOx, GeS2 and Se). Due to this pliability, the surface of the nanocrystalline sublayers of CdSe and ZnSe is expected to smooth out on a short scale. As can be seen in Fig. 9, there is a trend for Rms to grow with the layer thickness, although the experimental points are fairly dispersed, and this increase is smaller than that reported for ZnSe-based materials

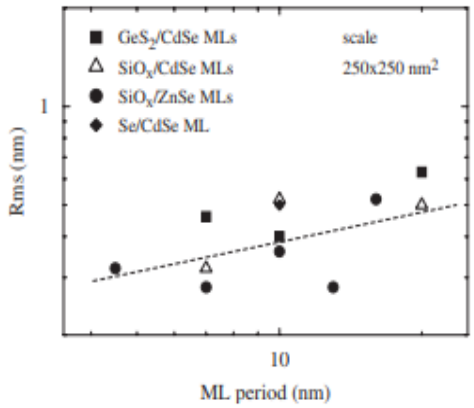

Fig. 9 Root mean square surface roughness (Rms) for 250 250 nm2 length scale versus the period of all MLs studied. The dashed lines are guides to the eye.

MLs at a scale of 3:4 4 mm2. Given the recent discovery of various b-values, our finding is compatible with those findings. Rms values (and thus interface thicknesses) of p1 nm obtained for all "step-by-step" deposited MLs studied here are significantly lower than those typical for MLs deposited in a single step by thermal evaporation in vacuum. HRTEM images clearly show SiO123 nm=SiO2 223 nm amorphous MLs generated by one-step deposition (i.e. without pausing the deposition of each layer of the ML) of thermally evaporated SiO in an oxygen atmosphere.

These results show that the step-by-step deposition method has a significant advantage over the one-step method; it allows for the formation of smooth single layers as well as the formation of amorphous and amorphous/nanocrystalline multilayers with smooth interfaces and very good artificial periodicity via thermal evaporation. The step-by-step approach may be useful when using alternative vapour deposition processes like as sputtering, glow discharge deposition, or chemical vapour deposition.

X-ray diffraction (XRD) was used to investigate the periodicity and interface sharpness of Se/CdSe aMLs as well as a-SiOxCdSe MLs (XRD). The obtained results reveal that both types of multilayers display significant artificial periodicity. The interface thickness of Se/CdSe a-MLs is 1.3 nm, according to an X-ray diffraction study. SiOx=CdSe=SiO HRTEM measurements of x three-layer structures (see Fig. 6) revealed that the layers of both types are continuous, smooth, and uniform in thickness on a scale of 200 nm, whereas the CdSe layers are nanocrystalline.

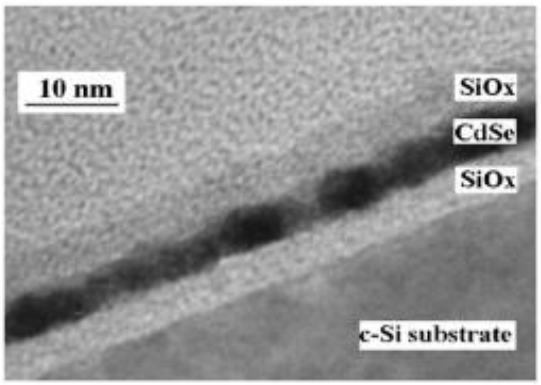

Fig. 10. HRTEM cross section micrograph of a SiOxð5 nmÞ=CdSeð5 nmÞ= SiOxð5 nmÞ three layer structure.

Regardless of whether the SiOx layers are amorphous. The contact has an average thickness of 1 nm. These results support the idea of using AFM to learn about the sharpness of the interface between SiOx=ZnSe and GeS2=CdSe MLs, as they are consistent with the AFM data obtained in this study for SiOx=CdSe and Se/CdSe MLs.

Normally, thin film surface roughness is created by steps caused by any substrate defect and, more importantly, by one or more layers of islands and pits (vacancy islands) caused by kinetic and/or thermodynamic factors during growth. Roughness in the shape of islands, pits, jagged terrace edges, and so on suggests that at the substrate temperature utilized, adatom and vacancy diffusion rates are too slow to keep up with deposition rates. Of our example, all layers in multilayers were created using the same deposition method and substrate temperature (300 K), but at different deposition rates, which, together with composition, can have a significant

impact on the adatom diffusion rate. X-ray diffraction results on Se/CdSe amorphous MLs demonstrate that, for MLs made of the same material pair, the faster the deposition rate, the thicker the interface. SiOx layers are deposited at a rate of 3.0 nm/s in SiOx=CdSe MLs and at a rate of 0.2 nm/s in SiOx=ZnSe MLs (see Experimental details for more information). The composition appears to be the most important factor, but the substantial difference in deposition rates between SiOx=CdSe and SiOx=ZnSe MLs (Fig. 10), could also play a role. Furthermore, preliminary observations on the surface morphology of as-deposited and many years' 'old' CdSe single layers show that, whereas as-deposited CdSe layers are smooth, the surface of the 'old' CdSe layers has hillocks and deep troughs in some areas. The hillocks reach heights of tens of nanometers. Some SiOxGeS2=CdSe MLs have been discovered to have similar (but not as high) hillocks on their surfaces. The production of such hillocks could explain the observed steep Rms increase in SiOxGeS2=CdSe MLs with increasing scan length, but the reason for their formation and composition remain unknown and will be thoroughly researched in the future.

5. CONCLUSION

However, the goals of reproductive medicine go well beyond simply easing the process of becoming pregnant and giving birth. It is not just a challenge in reproductive medicine that the current diagnostic and therapeutic options for many chronic diseases that result in a significant reduction in quality of life and/or infertility do not meet the requirements of a 'gold standard' of care. Low complexity, low risk, high diagnostic value, early preclinical disease diagnosis accuracy, few side effects, and high therapeutic efficacy are typical examples of these qualities. As a result of the widespread belief that diagnosing and treating reproductive pathologies will require surgical intervention at some point, numerous research groups are actively investigating the potential for non-invasive detection and treatment of minimally invasive reproductive pathologies. The use of systemic biomarkers has been attempted for the non-invasive detection of several'surgical' reproductive conditions, including endometriosis, uterine fibroids, ectopic pregnancy, and, to the greatest extent, gynecological/andrological malignancies. Diagnostic accuracy of biomarker-based techniques, however, has not been adequately demonstrated in many studies, limiting their application in clinical practice. The diagnostic accuracy of noninvasive imaging techniques like ultrasound, computed tomography (CT), and magnetic resonance imaging (MRI) is also being studied in depth, as is the possibility of increasing the selectivity of pharmacological drugs focused at the reproductive system (MRI).

The main current research directions in reproductive medicine are focused on enhancing the efficacy and precision of diagnostic and therapeutic methods, as well as the development of robust and targeted research tools, so it is not surprising that the number of attempts to apply nanotechnology principles to reproductive medicine and biology has steadily increased in recent years. The implementation of nanomaterial-based techniques, with their unparalleled robustness and targeting capabilities, is anticipated to contribute to the creation of next-generation diagnostic and therapeutic modalities to improve patient care, as has been the case in other areas of medicine.

REFERENCES

1. Nasrollahzadeh, M., Issaabadi, Z., Sajjadi, M., Sajadi, S. M., & Atarod, M. (2019). Types of nanostructures. Interface science and technology, 28, 29-80.
2. Pokropivny, V. V., & Skorokhod, V. V. (2008). New dimensionality classifications of nanostructures. Physica E: Low-dimensional Systems and nanostructures, 40(7), 2521-2525.
3. Belenkov, E. A., & Greshnyakov, V. A. (2013). Classification schemes for carbon phases and nanostructures. New Carbon Materials, 28(4), 273-282.
4. Stoner, B. R., & Glass, J. T. (2012). Carbon nanostructures: A morphological classification for charge density optimization. Diamond and related materials, 23, 130-134.
5. Gajanan, K., & Tijare, S. N. (2018). Applications of nanomaterials. Materials Today: Proceedings, 5(1), 1093-1096.

6. Khot, L. R., Sankaran, S., Maja, J. M., Ehsani, R., & Schuster, E. W. (2012). Applications of nanomaterials in agricultural production and crop protection: a review. Crop protection, 35, 64-70.
7. Gao, J., & Xu, B. (2009). Applications of nanomaterials inside cells. Nano Today, 4(1), 37-51.
8. Mandal, G., & Ganguly, T. (2011). Applications of nanomaterials in the different fields of photosciences. Indian Journal of physics, 85(8), 1229-1245.
9. Sharma, V. P., Sharma, U., Chattopadhyay, M., & Shukla, V. N. (2018). Advance applications of nanomaterials: a review. Materials Today: Proceedings, 5(2), 6376-6380.
10. Bratovcic, A. (2019). Different applications of nanomaterials and their impact on the environment. International Journal of Material Science and Engineering, 5(1), 1-7.
11. Lara, S., & Perez-Potti, A. (2018). Applications of nanomaterials for immunosensing. Biosensors, 8(4), 104.
12. Ghasemzadeh, G., Momenpour, M., Omidi, F., Hosseini, M. R., Ahani, M., & Barzegari, A. (2014). Applications of nanomaterials in water treatment and environmental remediation. Frontiers of environmental science & engineering, 8(4), 471-482.
13. Chen, H., Zeng, Y., Liu, W., Zhao, S., Wu, J., & Du, Y. (2013). Multifaceted applications of nanomaterials in cell engineering and therapy. Biotechnology advances, 31(5), 638-653.
14. Shafiq, M., Anjum, S., Hano, C., Anjum, I., & Abbasi, B. H. (2020). An overview of the applications of nanomaterials and nanodevices in the food industry. Foods, 9(2), 148.
15. Qiu, X., Zhang, Y., Zhu, Y., Long, C., Su, L., Liu, S., & Tang, Z. (2021). Applications of nanomaterials in asymmetric photocatalysis: recent progress, challenges, and opportunities. Advanced Materials, 33(6), 2001731.
16. Wang, W., Liao, S., Zhu, Y., Liu, M., Zhao, Q., & Fu, Y. (2015). Recent applications of nanomaterials in prosthodontics. Journal of Nanomaterials, 2015.
17. Barkalina, N., Charalambous, C., Jones, C., & Coward, K. (2014). Nanotechnology in reproductive medicine: emerging applications of nanomaterials. Nanomedicine: Nanotechnology, Biology and Medicine, 10(5), e921-e938.